BIOLOGICAL EVALUATION OF MITO-SG1 AS A POTENT CYTOTOXIC AGENT IN THE TREATMENT OF GASTRIC CANCER

Data de aceite: 01/08/2023

Giovanni A. Lineros-Franco
Translational Biomedical Research Group, Fundación Cardiovascular de Colombia, Floridablanca, Colombia.
Graduate Program in Biomedical Sciences, Faculty of Health, Universidad del Valle, Cali, Colombia.

Yenny Bueno-Duarte
Translational Biomedical Research Group, Fundación Cardiovascular de Colombia, Floridablanca, Colombia.

Julio Montoya-Villegas
Graduate Program in Biomedical Sciences, Faculty of Health, Universidad del Valle, Cali, Colombia.

Micael Hardy
Aix Marseille University, CNRS, ICR, SREP Team, Marseille, France.

Olivier Ouari
Aix Marseille University, CNRS, ICR, SREP Team, Marseille, France.

Marcos Lopez
Chemistry Department, University of Puerto Rico-Humacao, Puerto Rico

Sandra Sanabria
Translational Biomedical Research Group, Fundación Cardiovascular de Colombia, Floridablanca, Colombia.
Graduate Program in Biomedical Sciences, Faculty of Health, Universidad del Valle, Cali, Colombia.
Innovation and Technological Development Directorate. Fundación Cardiovascular de Colombia, Floridablanca, Colombia.
Tissue Bank Scientific Technical Directorate. Fundación Cardiovascular de Colombia, Floridablanca, Colombia.

ABSTRACT: Gastric cancer (CG) ranks third in cancer deaths and fifth in new cases each year in the world. In Colombia, CG has reached first place in deaths and third place in new cases each year. Recent studies have reported factors that lead to its development, great genetic variety, high concentration of reactive oxygen species (ROS), hyperpolarization of the membrane, lower oxygen consumption, and greater glycolysis compared to healthy gastric epithelial cells; in addition, mitochondrial dysfunction that promotes cell migration and accelerates invasion through ROS. New compounds called “mito-compounds” have

been designed to act on these factors to induce cell death by apoptosis. Mito-SG1 is a mito-compound that showed antitumor effects in triple-negative breast cancer. We evaluated Mito-SG1 in AGS (adherent CG cell line) and KATO III (semi-adherent CG cell line). Mito-SG1 inhibited cell growth, induced a concentration-dependent change in mitochondrial membrane potential (Δψm), and increased ROS production. It was seen in real time that Mito-SG1 significantly decreased mitochondrial bioenergetics of AGS and KATO III in a dose-time-dependent manner. Mito-SG1 induced cell death by intrinsic apoptosis. Mito-SG1 may be an alternative in the treatment of CG and may be used concomitantly with 5-Fluorouracil (5-FU) and Sorafenib.
KEYWORDS: Mito-SG1, Gastric Cancer, Mitochondria, Selective Treatment

1 | INTRODUCTION

CG is one of the leading causes of death in the world every year. GLOBOCAN reported that in 2.020 Was 1.089.103 new cases and 768,793 deaths from CG, ranking fifth in incidence and fourth in mortality, respectively. Asia is the region with the highest incidence (819,944) and mortality (575,206) by CG each year; while Latin America and the Caribbean rank third in both incidence (67,617) and mortality (53,392) each year. In Colombia, GC ranked fourth in incidence with 8,214 new cases, and first in mortality with 6,451 cases (Sung et al., 2021). Early detection of CG is essential to perform surgery as a first-line treatment; this is difficult because CG is usually asymptomatic until advanced stages are reached (Refolo, Lotesoriere, Lolli, Messa, & D'Alessandro, 2020). Treatment with the highest 5-year survival rate is surgical resection with chemotherapy which reaches 40%; the percentage varies according to the stage (Tan et al., 2020). In advanced stages, the treatment that includes surgery and the use of adjuvants such as chemotherapy, radiotherapy, or immunotherapy, has a 5-year global survival rate of less than 10% (Gonzalez-Hormazabal et al., 2019). This one is worse in individuals with advanced CG with a median survival of ~1 year. Poor prognosis is often explained by a lack of biomarkers, early diagnoses, and effective treatments. Numerous Studies have shown that these cells have higher glucose consumption than non-tumor cells even in the presence of oxygen and with biochemically active mitochondria, "Warburg effect" (Galluzzi et al., 2010). Vander Heiden et al, propose that tumor cell uses glucose as a carbon source in anabolic processes necessary for cell proliferation and synthesis of biomolecules used in multiple functions (Battogtokh, G., Cho, Y. Y., Lee, J. Y., Lee, H. S., & Kang, 2018; Neuzil, Dong, Rohlena, Truksa, & Ralph, n.d.). ROS dynamically influences the tumor microenvironment; Despite playing a fundamental role in healthy cellular metabolic processes, high concentrations can increase tumorigenesis or lead to apoptosis (W Y Hung et al., 2012; Shen et al., 2014). The mitochondrial membrane of tumor cells has been reported to be hyperpolarized (-140 mV to -180 mV) (Cheng et al., 2011; Cunniff et al., 2014). This was corroborated in human gastric cancer cell lines (AGS) with high concentrations of Ca2+ (Kalyanaraman, 2017). Search for successful and novel therapies that inhibited some of the factors discussed above allowed

the development of drugs with the mitochondrial activity called mitochondrial compounds that have shown selective toxicity against tumor cells due to Δψm. These compounds are synthesized bound to the triphenylphosphine cation (TPP^+) by a 10-carbon aliphatic side chain that helps their orientation and accumulation within the mitochondrial matrix (Herzig & Shaw, 2018; Lee, Jung, Jung, Heo, & Jeong, 2016; Pauligk et al., 2017; Vlq, Ri, Lgdwlyh, Ri, & Santos, 2012). Mito-SG1 is a linear nitroxide (SG1 [(N-tert-butyl-N-[1-diethylphosphono-(2,2- dimethylpropyl)]] conjugated to TPP^+). Nitroxides mimic superoxide dismutase (SOD); have the potential to scavenge reactive free radicals and inhibit ROS-producing mechanisms such as Fenton and Haber-Weiss reactions (KIM, MIN, & LEE, 2020); They decrease survival signaling and induce apoptosis. Studies *in vitro* in triple-negative breast cancer and liver showed that Mito-SG1 at the maximum mean inhibitory concentration (IC_{50}) micromolar affected mitochondrial bioenergetics, colony formation, proliferation, and migration, demonstrating selective cytotoxic effects (Vlq et al., 2012). There are no studies that explain the mechanisms of Mito-SG1 activity in CG. Considering the hyperpolarization of the mitochondrial membrane showed in CG, it is expected that Mito-SG1 inhibiting their bioenergetics, with possible effects on MAPK pathways, PPARγ and PI3K/Akt, and that produces cell death by apoptosis.

2 | MATERIALS AND METHODS

2.1 Cell culture

Cell lines were bought from American Type Culture Collection (ATCC) (Manassas, USA). HPSEC was maintained with a Complete Human Epithelial Cell Medium/w-500 mL kit (Cell Biologics, Cat#H6621), AGS remained in Ham's F-12 Kaightn's Modification (Caisson, Ref: HFP06-50LT) and KATO III remained in Medium Modified from Dulbecco de Iscove's (Caisson, Ref: IMP03-50LT) supplemented with Fetal Bovine Serum (SFB) 10% (Biowest, Material: S181B-500), sodium bicarbonate 1.5 g/L and antibiotics (100 U/ml of penicillin and streptomycin) at 37°C and 5% CO2.

2.2 MTT cytotoxicity test

MTT (3-(4,5-dimethylthiazol-2-yl)-2,5-diphenyltetrazolium bromide) (Mosmann, 1983) was used to evaluate the cytotoxicity of Mito-SG1, SG1, and TPP^+. Cells were seeded into 96-well plates as follows: HPSEC ($4 \times 10^4\ cells/well$), AGS ($1{,}5 \times 10^4\ cells/well$), and KATO III ($5 \times 10^4\ cells/well$); incubated overnight, and then treated with Mito-SG1, SG1, and TPP^+ (0.1, 0.3; 1; 3, 10, and 30 µM) for 24, 48, and 72 h in individual trials. The culture medium was then removed from each well and 100 mL of fresh media supplemented with MTT (50 mg/mL) was added; plates were covered with aluminum foil and incubated for 2 h at 37°C and 5% CO_2. Then, MTT was removed and 100 µL of DMSO was added, the plate

was left stirring for 20 minutes. Absorbance reading was performed in the Varioskan Flash Spectral Scan (Thermo Fisher Scientific, Waltham, MA, USA) plate reader at (λ=595 nm).

2.3 Colony formation test

Cells were seeded in plates of 6 wells, HPSEC (3 x 10^2 $cells/well$), AGS (4 x 10^2 $cells/\ well$), and KATO III (5 x 10^2 $cells/well$) were cultured for 24 h in 1.5 mL of culture medium at 37°C and 5% CO_2. KATO III, being semi-adherent, foresaw the planting, a process of preparation of sterile wells was conducted with 2 mL of gelatin-based coating solution (Cell Biologics, Catalog No. 6950) for 2 minutes so that cells adhere to the plaque and prevent their loss in culture medium changes and washes. 24 h after incubation, all cell lines were removed from the culture medium to apply Mito-SG1, SG1, and TPP^+ (0.1, 0.3; 1; 3; 10 and 30 µM) for 24 h; in KATO III, Prior, culture dish was centrifuged at 900 g for 5 minutes. Then, a change of culture medium is made by fresh culture medium, 3 days later process is repeated until reaches at least 50 cells in the colonies (9 days). Wells were washed 3 times with preheated phosphate-buffered saline (PBS) and stained with 4% violet- paraformaldehyde crystal solution for 30 min. Cells were washed with type II water; when wells were dry, colonies were counted in the VersaDoc™ equipment with QUANTITY ONE software. Colony formation efficiency (CF) and survival fraction (FS) were calculated (Annex 4).

2.4 Detection of cell death with SYTOX® Green assay

Cell death assessment was performed in real-time with SYTOX® Green (Invitrogen) probe. Cells were seeded in black plates of 96 wells, HPSEC (4 x 10^4 $cells/well$), AGS (1,5 x 10^4 $cells/well$), and KATO III (5 x 10^4 $cells/well$) at 37°C and 5% CO2. After 24 h of incubation, cultures were treated for 24 h with different concentrations of Mito-SG1 (0.1; 0.3; 1; 3; 10, and 30 µM) in the presence and absence of SYTOX® Green; They were prepared for AGS and KATO III (0.5 µM) and HPSEC (0.75 µM). TRITON 100X was used as a positive control of cell death. Some wells were used as a control with SYTOX® Green and others without any treatment as a control of the assay. Immediately, fluorescence was measured in the plate reader ($\lambda_{abs}/\lambda_{emi}$=504/523 nm). Fluorescence measurement was performed for 24 h, first 2 h, reading was made every 15 minutes, next hour was done every 30 minutes, then it was done every hour until reaching 6 h, from this moment it was done every 6 h. Plates were kept at 37°C and 5% CO2; were only removed from the incubator for reading.

2.5 Cell migration assay (Wound Healing)

AGS (1,5 x 10^4 $cells/well$) was sown in plates of 24 wells and incubated at 37°C and 5% CO_2 until reaching 100% confluence; Then, a wound was made in a straight line in

the monolayer with a yellow pipette tip; wells were flushed three times with preheated PBS to remove floating cells. Cells were then treated with Mito-SG1 (0.5; 1 and 1.5 µM), and the culture medium was changed every 24 h with a fresh treatment-free medium to remove floating cells. The trial ended when the wound closed in the control wells. Images were taken (0, 24, 48, and 72 h) after the wound was performed (Annex 5). Images were analyzed with the free software T-Scratch (www.cse-lab.ethz.ch/software.html)

2.6 Evaluation of apoptosis

AGS and KATO III were treated with Mito-SG1 (2 and 3 µM) for a period of 48 h in 100 mm Petri dishes, apoptosis/necrosis detection kit (Abcam) was used. After collecting cells, they were stained with Apopxin Green, 7-AAD, and violet CytoCalcein 450 for 60 min in total darkness; cells (5 x 10^5 $cells/mL$) were analyzed in the flow cytometer FACSCanto II (Becton Dickinson, Heidelberg, Germany).

2.7 Evaluation of mitochondrial transmembrane potential (Δψm) (TMRE)

HPSEC (4 x 10^4 $cells/well$), AGS (1,5 x 10^4 $cells/well$), and KATO III (5 x 10^4 $cells/well$) were planted in black plates 96 flat-bottomed wells, treated with Mito-SG1 (0.5, 1 and 2 µM) for 24 h at 37°C and 5% CO_2. The culture medium was removed, and two washes were carefully performed with tempered PBS, 100 µL of TMRE solution (800 nM) was added and incubated for 30 minutes; the positive control was FCCP (30 µM). Fluorescence was measured in the plate reader ($\lambda_{abs}/\lambda_{emi}$=488/575 nm).

2.8 Evaluation of Caspase Activity 3/7

AGS and KATO III were treated with Mito-SG1 (1 and 2 µM) for 48 h in an incubator at 37°C and 5% CO_2. Cells were labeled with a caspase 3/7 kit (C10427, Thermo Fisher Scientific). Trypsinized cells were collected and green detection reagent CellEvent™ Caspase-3/7 was added and incubated for 30 min at 37ºC in total darkness. Caspase activity was analyzed in the FACSCanto II flow cytometer (Becton Dickinson, Heidelberg, Germany).

2.9 Cytochrome c release assay

AGS and KATO III were treated with Mito-SG1 (2 µM), and Mitochondria Isolation Kit for cultured cells (Pierce) was used according to the manufacturer's instructions. Isolated cells and mitochondria were lysed in iced lysis RIPA buffer (Tris-HCl (25 mM), NaCl (150 mM), NP40 (1% (w/v), sodium deoxycholate (1% (w/v)), SDS (0.1% (*w/v*)), sodium

orthovanadate (1 mM), sodium fluoride (3 mM), and protease inhibitor cocktail (50 mM) (Amresco). Protein concentration was measured with PierceTM BCA assay (Thermo Fisher Scientific, Rockford, IL 61101, USA) 18 µg of protein was loaded into a 14% SDS-PAGE and transferred to a polyvinylidene difluoride membrane. Membranes were probed with specific antibodies to β-actin (SC-8432), cytochrome c (D18C7), and COX IV (3E11) and bought from Cell Signaling Technology (Beverly, MA). As a secondary antibody was used goat anti-rabbit IgG-HRP (A02208). Protein quantification was performed using Image J (www.rsb.info.nih.gov). Densitometry reading of bands was normalized according to actin expression. Primary antibodies were added for 16 h at 4°C and secondary antibodies for 1 h at 24°C. Antibody binding with SuperSignal™ West Pico Chemiluminescent Substrate (Pierce) was detected.

2.10 Apoptosis Detection (TUNNEL)

Apoptotic cells were detected using APO-BrdU TUNEL (Invitrogen) assay kit. AGS and KATO III were collected 48 h after treatment with Mito-SG1 (2 and 3 µM) and at once fixed to 1% paraformaldehyde. Cells were incubated in DNA labeling solution (TdT and BrdUTP) for 3 h at 37°C, washed, and incubated with labeled Alexa Fluor 488 anti-BrdU antibodies for 30 min at room temperature. Cells were then analyzed by the FACSCanto II flow cytometer (Becton Dickinson, Heidelberg, Germany).

2.11 Evaluation of cell signaling pathways

AGS and KATO III were treated with Mito-SG1 (2 µM) for 24 h at 37°C. Isolated cells and mitochondria were lysed in icy lysis RIPA buffer (Tris-HCl (25 mM), NaCl (150 mM), NP40 (1% (w/v)), sodium deoxycholate (1% (w/v)), SDS (0.1% (w/v)), sodium orthovanadate (1 mM), sodium fluoride (3 mM), and protease inhibitor cocktail (50 mM) (Amresco). Protein lysates were centrifuged at 15000 g for 15 min at 4°C to remove insoluble material; protein concentration was decided by PierceTM BCA assay (Thermo Fisher Scientific, Rockford, IL 61101, USA). Proteins were separated in SDS-PAGE and transferred to a polyvinylidene difluoride membrane. Membranes were probed with specific antibodies against β-actin, p-AMPK (40H9), B-Raf (55C6), PPAR-γ (81B8), MEK 1/2 (47E6), p-MEK 1/2 (41G9), c- Raf (9422), Ras (27H5), Erk 1/2 (137F5), p-Erk 1/2 (197G2), p-LKB1 (C67A3), KLB1 (D60C5), p-ACC (3661), p-AKT (D9E), p-PI3K (4228) purchased from Cell Signaling Technology (Beverly, MA). Anti-rabbit Goat probe IgG-HRP (A02208) was used as a secondary antibody. Signals were evaluated using SuperSignal™ West Pico Chemiluminescent Substrate (Pierce) (Annex 24).

2.12 Mitochondrial Superoxide Evaluation, (Mito-SOXTM Red)

Cell cultures trypsinized when confluence reached 70 to 80%. Cell density and ideal concentrations of Mito-SOX™ Red (Invitrogen, Creek Road, Eugene, USA) probe were decided. $O2^{\cdot-}$ production was measured with Mito-SOX™ Red. AGS ($1{,}5\ x\ 10^4\ cells/well$) and KATO III ($5\ x\ 10^4\ cells/well$) were grown in 96-well black plates at 37°C and 5% CO_2. They were treated with Mito-SG1 (1, 2, 3, and 5 µM) for 48 h. The medium was then removed from wells and a Mito-SOXTM Red (4 µM) solution was added and incubated for 30 min at 37°C, then gently washed three times with PBS. Immediately, fluorescence was measured in the plate reader ($\lambda_{abs}/\lambda_{emi}$=510/580 nm).

2.13 Evaluation of Hydrogen Peroxide, (Amplex red)

AGS ($1{,}5\ x\ 10^4\ cells/well$) and KATO III ($5\ x\ 10^4\ cells/well$) were cultured in 96-well black plates at 37°C and 5% CO_2, treated with Mito-SG1 (1, 2 and 3 µM) for 24h, then washed once with PBS and incubated in Amplex Red (100 µM) and HRP 0.25 (U/mL) solution prepared in PBS. After 30 min, fluorescence was measured in the plate reader ($\lambda_{abs}/\lambda_{emi}$=540/580 nm). H_2O_2 formation was quantified using a standard curve of known H_2O_2 concentrations.

2.14 Superoxide Dismutase (SOD) Evaluation

SOD was measured with Trevigen, Inc. Superoxide Dismutase Kit (Gaithersburg, MD, USA). Protein extract was used to assess total SOD activity. SOD reaction buffer was mixed with Xanthine solution followed by a solution of Nitro Blue Tetrazolium (NBT). Proteins were isolated 24 h after treatment with Mito-SG1 (2 and 3 µM), and absorbance was set to zero at (λ=550 nm). Then, Xanthine oxidase solution was added, and readings were taken at (λ=550 nm) on a Multiskan go spectrophotometer (Thermo Scientific) every 30 s for 5 min. Total SOD activity was calculated based on the manufacturer's formula.

2.15 Evaluation of affectation on mitochondrial bioenergetics

The effect of Mito-SG1 on mitochondrial bioenergetics of cells was evaluated in real-time with a Seahorse XFe24 analyzer (Seahorse Bioscience, North Billerica, MA, USA). Measurements were normalized to protein content using the Bradford method.

- ***Mito Stress Test***

Mito Stress Test evaluates the effect produced by the drug of interest on integrated cellular oxygen consumption rate (OCR). Using mitochondrial inhibitors, basal respiration, maximal respiration, ATP production, proton leakage, reserve capacity, and non-mitochondrial respiration were evaluated in pretreated and untreated cells. Cells were seeded in 100 µL

of solution in Seahorse XFe24 plates from 24 wells, HPSEC (5 x 10^4 $cells/well$), AGS (7 x 10^4 $cells/well$), and KATO III (6 x 10^4 $cells/well$) at 37°C and 5% CO_2. Four wells were used as control according to supplier protocol. Cells were incubated at 37°C and 5% CO_2 until they adhered to the plate. For KATO III, the plate was first centrifuged at 1000 g for 5 min, processes that are repeated each time the medium is removed to prevent cell loss. Cells were treated with Mito-SG1 (0.5; 1 and 2 µM) in 150 µL which is gently added to each well to complete a final volume of 250 µL (This procedure is the same for all bioenergetic tests). After 24 hours of incubation, wells were washed following the supplier's protocol, 200 µL of the medium was removed from each well, then 600 µL of SFB-free Seahorse DMEM medium, and sodium bicarbonate was added, supplemented with glucose (25 mM), pyruvate (1mM) and glutamine (2 mM), and pH adjusted to 7.4. Then, 600 µL of the medium was removed from each well, and the same volume of fresh medium was added to them, this volume was removed once again, and 450 µL of the medium was added to complete 500 µL of the final volume. The plate was left for 45 minutes at 37ºC free of CO_2. During this time, inhibitors of mitochondrial complexes were prepared and deposited in the cartridge ports as follows: 75 µL of Oligomycin (1.25 µM) in ports A, 75 µL of FCCP (0.5 µM) in ports B, and 75 µL of Rotenone/Antimycin A (1.0 µM) in ports C. Inhibitors are added to wells sequentially by previously programmed equipment.

- ***Phenotype assay***

This assay is used to evaluate the pharmacological effect on OCR and extracellular acidification rate (ECAR) of cells. Results are indicators of mitochondrial respiration and glycolysis at baseline and stress; These values are used to report cellular energy metabolism, basal phenotype, stressed phenotype, and metabolic potential. The procedure is the same as that performed with Mito Stress Test.

- ***Glycolytic Rate Assay***

This assay evaluates cellular aerobic glycolysis by measuring RCT at baseline and compensatory glycolysis after mitochondrial inhibition. Basal glycolysis, basal proton efflux rate, compensation glycolysis, and post-2-DG acidification were evaluated. After 24 h of treatment with Mito-SG1 (0.5; 1 and 2 µM) at 37°C and 5% CO_2, first washing was carried out and the plate is taken to the CO_2-free incubator for 45 minutes, during this period inhibitors were prepared, in ports A of the cartridge was deposited 75 µL of glycolysis inhibitor 2-DG (50 mM), and in ports B 75 µL of Rotenone/Antimycin A (1 µM). Then, a second wash was performed and 475 µL of DMEM medium was gently added completing a final volume of 525 µL and taken to the equipment.

- ***Mito Fuel Test)***

This assay evaluates the dependence, flexibility, and ability of cells to try to counteract affectation produced by Mito-SG1 (0.5 µM) in a final volume of 250 µL into the well. After 24

h of incubation at 37°C and 5% CO_2, washes were performed with Seahorse DMEM medium free of SFB and sodium bicarbonate, supplemented with glucose (10 mM), pyruvate (1 mM) and glutamine (2 mM) and pH adjusted to 7.4. Inhibitors were prepared according to a metabolic pathway to be evaluated, e.g., glutamine inhibition, a volume of 56 µL BPTES (3 µM) was prepared, and a mixture was prepared with those of other inhibitors in a volume of 62 µL Etomoxir (4 µM)/UK-5099 (2 µM).

2.16 Evaluation of synergy between (Mito-SG1 and antitumor drugs used in the treatment of CG)

The effect of treatments prepared equimolarly between Mito-SG1 and GC antitumor drugs (Doxorubicin (DXR), Sorafenib, and 5-FU) was evaluated 48 h later with MTT. Dose-response curves and synergy were calculated based on the Chou Talalay method with CALCUSYN software.

2.17 Statistical analysis

Trials were conducted in triplicate independent trials; results were analyzed and expressed as the standard error of the mean (SEM). Analysis of variance (one-way ANOVA) and Tukey's test were performed. All graphics were designed in GraphPad Prism 8.0

3 I RESULTS

3.1 Mito-SG1 inhibits cell viability and induces cell death in AGS and KATO III

Mito-SG1 (0.1, 0.3; 1; 3; 10 and 30 µM) affected cell viability in a dose-time-dependent manner, IC_{50} at 24, 48 and 72 h in AGS were (3.35; 1.29 and 0.76 µM) respectively, IC_{50} in HPSEC were (2.88; 1.75 and 1.71 µM) respectively, and in KATO III, the IC_{50} at 48 and 72 h were (1.52 and 0.48 µM) respectively (Figure 1A). Mito-SG1 at 24 h mainly affected HPSEC, but, at 48 and 72 h the effect was greater in AGS and KATO III. SG1 did not affect any cell lines. TPP^+ (30 µM) affected cell lines significantly, with a concentration higher than IC_{50} of Mito-SG1 in cell lines (Figure 1B). Colony formation assay showed that SG1 and TPP^+ did not affect cell lines (Figure 1C). Mito-SG1 strongly affected AGS (IC_{50}= 1.7 µM), compared to KATO III (56.78 µM). Involvement in HPSEC (IC_{50}= 31.8 µM) was ~30 times lower than in AGS, contrary to that seen with MTT (Figure 1D). SYTOX® Green showed that Mito-SG1 (1; 3; 10 and 30 µM) significantly affected AGS in a dose-dependent manner proving that KATO III is more resistant to treatments during the first 24 h (Figure 1E). Wound healing trial in AGS showed that Mito-SG1 (0.5; 1 and 1.5 µM) has a significant dose-time dependent effect on metastasis (Figure 1F).

3.2 Mito-SG1 strongly affects mitochondrial integrity in AGS and KATO III leading to cell death by apoptosis.

Mito-SG1 (1 and 2 μM) led to mitochondrial membrane depolarization significantly in a dose-dependent manner in AGS and KATO III (Figure 2A). Amplex Red probe showed that Mito-SG1 (3 μM) produced a significantly reduced concentration of H_2O_2 in KATO III in a dose-dependent manner; no significant differences were seen in AGS although there was involvement of Δψm (Figure 2B). Mito-SG1 (2, 3, and 5 μM) significantly affected dose-dependent $O2^{\cdot-}$ production (Annex 7) in AGS, but not in KATO III, as seen at H_2O_2 levels (Figure 2C). To corroborate these effects on ROS, we evaluated whether there were changes in SOD concentration. Mito-SG1 (2 and 3 μM) significantly increased SOD activity in a dose-dependent manner in KATO III; in AGS an increase was seen with Mito-SG1 (3 μM), an unexpected result concerning the evaluation of ROS with Mito-SG1 (3 μM) (Figure 2D). Apopxin stain showed that Mito-SG1 (1 and 2 μM) for 48 h in AGS increased the percentage of apoptotic cells significantly in a dose-dependent manner concerning the control by up to 8 times, while in KATO III the increase was 2 times greater to the control (Figure 2E). Western Blot analysis showed that Mito-SG1 (2 μM) in KATO III increased cytochrome c release by up to ~225% (Figure 2F). Flow cytometry showed that Mito-SG1 (1 and 2 μM) for 48 h in AGS significantly increased dose-dependent levels to 95% presence of caspases 3/7. In KATO III Mito-SG1 (2 μM) significantly increased levels in a dose-dependent manner to 35% (Figure 2G). Based on the above results, it is hypothesized that Mito-SG1 generated cell death through apoptosis. With the TUNEL probe, it was seen that Mito-SG1 (2 μM) for 48 h in AGS apoptosis occurred in ~45% of cells and KATO III, Mito-SG1 (2 and 3 μM) produced apoptosis in ~70% (Figure 2H). Results supplied important evidence that Mito-SG1 may be driving AGS and KATO III cells toward apoptosis via an intrinsic pathway.

3.3 Mito-SG1 induced AMPK activation and AKT suppression in AGS and KATO III

Evaluation of the effect of Mito-SG1 (2 μM) on the expression of signaling pathway proteins in AGS and KATO III showed significant differences.

- ***Ras/BRAF/CRAF/MEK/ERK Evaluation:***

In AGS an increase in the expression of Ras~30%, BRAF~35%, and CRAF~80% was seen; in KATO III, a significant increase in the expression of p-MEK/MEK ratio was seen by ~290% (Figure 3A).

- ***Evaluation of LKB1/AMPK/ACC pathway:***

In AGS, an increase in the expression of the p-AMPK/AMPK ratio was seen by ~160%; in KATO III, the expression of the p-ACC/ACC ratio was increased by ~40%. It is important to emphasize that it was seen that treatment in this cell line produced an increase

in expression that was not significant in AMPK, perhaps by trying to counteract the stress of treatment (Figure 3B).

- ***Evaluation of PI3K/Akt pathway:***

In AGS a non-significant increase in the expression of PI3K/Akt was seen, this may be an indicator that cells tried to respond to treatment as a form of resistance through this pathway. In KATO III, a non-significant reduction in p-Akt/Akt was seen that may have influenced the inability of cells to avoid apoptosis (Figure 3C).

- ***Evaluation of PPAR-γ pathway:***

In KATO III it reduced PPAR-γ expression by ~70%. Reduction in PPAR-γ expression may be related to the activity of Mito-SG1 on the MAPK pathway and low response by the cell despite a non-significant increase in AMPK expression. (Figure 3D).

3.4 Mito-SG1 affects mitochondrial bioenergetics in AGS and KATO III

Mito-SG1 (0.5; 1 and 2 μM) reduced OCR, ATP production, maximal respiratory capacity, respiratory reserve capacity, and non-mitochondrial respiration significantly in a dose- dependent manner and only affected electron leakage with the highest concentration. AGS was the most affected. In KATO III there was no involvement in proton leakage and HPSEC non-mitochondrial respiration was not affected (Figure 4A). Mito-SG1 (0.5; 1 and 2 μM) in AGS and Mito-SG1 (1 and 2 μM) in HPSEC increased the values of basal glycolysis, basal electron flow rate, and compensatory glycolysis not significantly, while in KATO III Mito- SG1 (0.5; 1 and 2 μM) reduced them (Figure 4B). Treatments significantly affected the OCR in a dose-dependent manner and metabolic potential mainly in AGS (Figure 4C). It was seen under stress conditions AGS and KATO III depend mainly on mitochondrial metabolism. Mito-SG1 (0.5 μM) caused greater mitochondrial disruption in AGS, and energy requirements were met by glycolysis. Mito-SG1 caused a significant change in glutamine dependence and to a lesser degree in dependence on fatty acids as carbon sources for oxidative phosphorylation. A significant decrease in glutamine flexibility alone was seen in SFA (Figure 4D).

3.5 Mito-SG1 potentiates the antineoplastic activity of 5-FU and Sorafenib in AGS and KATO III

AGS and KATO III were cultured in the presence of individual treatments with Mito-SG1, DXR, Sorafenib, 5-FU, and combinations of Mito-SG1 in the equimolar ratio (1:1) with each of them. Cytotoxicity was evaluated by MTT at 48 h of treatment (Figure 5A). The Chou- Talalay method was used to decide the type of effect of the combinations in AGS and KATO III. Isobolograms were designed and analyzed with Calcusyn software (Figure 5B). ED90 is used to know the combination index (CI) and the type of effect IC<1 (synergism),

CI=1 (additive), and CI>1 (antagonism) (Gonzalez-Hormazabal et al., 2019; H. Wang, Wang, Wang, Zeng, & Xing, 2022). Table 1 presents the effects of all treatments.

Treatment	AGS IC_{50} (μM)	KATO III IC_{50} (μM)	ED90 AGS	Effect	ED90 KATO III	Effect
Mito-SG1	1,477	1,516	-	-	-	-
DXR	0,130	0,904	-	-	-	-
Sorafenib	6,108	1,137	-	-	-	-
5-FU	52,411	59,883	-	-	-	-
Mito-SG1 : DXR (1:1)	0,113	0,731	0.90884	Additive effect	1.09936	Additive effect
Mito-SG1 : Sorafenib (1:1)	1,119	0,756	0.82358	Light synergism	0.87149	Light synergism
Mito -SG1 : 5-FU (1:1)	1,421	0,347	0.29642	Strong synergism	0.08956	Very strong synergism

Table 1. IC50 and effect of treatments on AGS and KATO III

4 I DISCUSSION

Mito-SG1 significantly affected cell viability in a dose-time-dependent manner; at 24 h mainly affected by HPSEC, and at 48 and 72 h the effect was greater in AGS and KATO III. SG1 had no effect. TPP^+ (30 μM) if it affected them at concentrations much higher than IC_{50} by Mito-SG1. Mito-SG1 inhibited colony formation, proliferation and migration of tumor cell lines evaluated demonstrating selective cytotoxic effects on tumor cells (Vlq et al., 2012). Mito-SG1 strongly affected AGS (IC_{50}=1.7 μM) compared to KATO III (56.78 μM) and in HPSEC was ~30 times lower (IC_{50}=31.8 μM), this value is extremely high compared to the results obtained with MTT. These differences highlight the importance of continuing to explore the potential of this Mito compound in other CG cell lines to assess selectivity by cancer cells. SYTOX® Green showed that AGS is more sensitive to Mito-SG1 (30 μM) compared to KATO III and HPSEC. Mito-SG1 (0.5, 1, and 1.5 μM) affect cell migration in AGS indicating the potential of Mito-SG1 on the metastatic capacity of these cells. Mito - SG1 induced cytochrome c release into the cytoplasm and activated caspase 3/7 in both AGS and KATO III. Mito-SG1 increased the percentage of apoptotic cells in AGS and KATO III; Therefore, our results supplied evidence that apoptosis Mito-SG1-induced can pass through the intrinsic pathway in both cell lines. Mito-SG1 affected the mitochondrial bioenergetics of these cells. It was seen with Western Blot that Mito-SG1 (2 μM) for 48 h affected differently the signaling pathways evaluated in AGS and KATO III.

- ***Evaluation of Ras/Raf/MEK/ERK pathway:***

Mito-SG1 affected the Ras/Raf/MEK/ERK pathway in AGS, a significant increase in Ras expression levels was seen by ~30%, this is probably due to the need to counteract

stress by activating genes that increase cell proliferation. An increase in BRAF expression was observed by ~35%, this protein is related to processes of cell differentiation, cell motility, and autophagy (Paskeh et al., 2022; W. Wang, Chen, Huang, & Juan, 2021); Studies have reported that inhibitors of this protein in melanomas can induce autophagy. Its inhibition in patients with advanced melanoma has significantly prolonged survival time (Lin et al., 2020). Mito-SG1 especially affected CRAF by increasing its expression by ~80%. Activation of this proto-oncogene starts a mitogen-activated protein kinase (MAPK) cascade. When RAF-1 is phosphorylated, it activates the cell death antagonist BAD/Bcl2. This promotes NF-kB activation and inhibits signal transducers involved in motility (ROCK2), apoptosis (MAP3K5/ASK1 and STK3/MST2), proliferation, and angiogenesis (RB1), can protect cells from apoptosis by translocating to the mitochondria, where it binds to BCL2 and displaces the antagonist BAD/Bcl2 from cell death, regulates Rho signaling and migration, and is necessary for normal wound healing (Tarasiuk, Miceli, & Domizio, 2022). Studies have reported the role of RAF-1 in cell cycle progression by ERK, it can also do so independently through the formation of a complex with the proteins Polo-Like kinase 1 (PLK1) and protein Aurora kinase A (Aurora A). PLK1 and Aurora A are important regulators of mitotic progression located in the mitotic spindle seen in tumor cells. This was confirmed by the researchers through the allosteric inhibitor KG5 that prevents the phosphorylation of RAF-1, therefore, the formation of the complex with PLK1, results in the arrest of mitosis in prometaphase. Hüser et al, reported that Knock out RAF-1 models increased apoptosis in embryonic tissues without having activated ERK (Lewandowski & Gwozdzinski, 2017). Our results in AGS may be related to the resistance of cells to counteract the apoptotic processes discussed above. The increase in RAF-1 in KATO III was not significant. An extraordinarily strong significant increase in the expression of the p- MEK/MEK ratio of ~290% and a non-significant increase in ERK were seen in KATO III; in AGS the increase was not significant in MEK/ERK. An increase in this ratio has been linked to chemoresistance in several types of cancer including CG (Boice, Bouchier-hayes, & Biology, 2020). This protein activated by MEK is translocated inside the nucleus regulating the expression of a large number of proteins, among this group are proteins associated with the plasma membrane such as CD120a (differentiation group 120), Calnexin; transcription factors that activate genes known as SRC-1 (steroid receptor coactivator-1) early response genes; NFAT (activated T-cell nuclear factor); MEF2 (myocyte enhancing factor-2); activator protein-1 (AP1/c-jun and c-fos); C-MYC (cellular homolog of avian myelocytomatosis virus oncogene); STAT3 (signal transducer and transcription-3 activator); cytoskeletal proteins (paxillin); RSK (protein kinases and phosphatase), (ribosomal kinase S6); MSK (mitogen- and stress-activated kinases); and epigenetic modifiers such as DNMT3B (cytosine-5-methyltransferase 3β). Most of these genes take part in the upregulation of CDKs (cyclins and cyclin-dependent kinases) and downregulation of regulators of cell cycle checkpoints p21 and p27. This shows that MEK/ERK axis increases the proliferation of differentiated cells, germ stem

cells, and cancer stem cells. ERK is, therefore, a fundamental regulator in the processes of proliferation, migration, and apoptosis. as well as an attractive therapeutic target in cancer (Moindjie, Rodrigues-Ferreira, & Nahmias, 2021). Overexpression of MEK in KATO III may be an indicator that this cell line may have some type of resistance to treatment. There are currently several treatments approved and under development to inhibit the overexpression of the MEK/ERK axis and thus inhibit the genetic factors mentioned above (Mast et al., 2020; Snezhkina et al., 2019).

- ***Evaluation of LKB1/AMPK/ACC pathway:***

Mito-SG1 in AGS significantly increased the expression of p-AMPK/AMPK by ~160%, in KATO III no significant differences were seen. Mito-SG1 produced in KATO III, a significant increase in expression of p-ACC/ACC in ~40%, this overexpression taking into account the activation, although it was not significant of AMPK in this cell line, is probably due to the increase in the concentration of pyruvate and/or acetate that allows achieving that activation and this should be directly related to the elevation in the reserve of fatty acids.

- ***Evaluation of PI3K/Akt pathway:***

Analysis showed no significant changes in the expression of p-PI3K/PI3K and p-Akt/Akt. PI3K/Akt pathway is critical in the regulation of cell growth, proliferation, metabolism, and angiogenesis. Deregulation of this pathway has a role in promoting GC (Salaroglio, Mungo, Gazzano, Kopecka, & Riganti, 2019). When Akt is active, it induces the activation of the mammalian target of rapamycin (mTOR) which in turn phosphorylates S6K1 and 4EBP1, favoring the transduction and synthesis of ribosomal and regulatory proteins of the cell cycle (Cheng, Y., & Tian, 2017). Inhibition of Akt, one of the main tumor suppressors, involved in the regulation of metabolism, in the uptake of glucose in muscle cells, its dysregulation is related to the development not only of cancer but also of other diseases such as diabetes, cardiovascular and neurological diseases (Ciccarese, Zulato, & Indraccolo, 2019). In AGS, an increase in PI3K/Akt expression was seen in the cells that received the treatment, although it was not significant if it can be an indicator that the cell tried to respond to the treatment as a form of resistance through this pathway. In KATO III, a non-significant reduction in p- Akt/Akt was seen that may have influenced the inability of cells to avoid apoptosis.

- ***Evaluation of PPAR-γ pathway:***

Peroxisome proliferator-activated γ receptor (PPAR-γ) is found primarily in adipose tissue. PPAR-γ participates in processes of differentiation and proliferation of adipocytes, in the capture and storage of fatty acids (FA), in the consumption of glucose, and in the activation of insulin (Batchuluun, Pinkosky, & Steinberg, 2022; Wen Yi Hung et al., 2012). Wu et al, observed in esophageal cancer cells that activation of PPAR-γ suppressed proliferation and induced apoptosis through inhibition of the MAPK pathway in esophageal cancer (Yu, Wu, Yao, & Tao, 2019). Recent studies reported on the possible activation of PPAR-γ mediated by short-chain and long-chain fatty acids that activate the proapoptotic enzyme 15- lipoxygenase (15-LOX). This can induce apoptosis in cancer cells via MAO-A (Riquelme et al., 2018).

They have also observed that some flavonoids such as Isorhamnetin, inhibited proliferation in CG cell lines (AGS and HGC-21) by mitochondria-dependent apoptosis by activating the PPAR-γ cascade (Matsuoka & Yashiro, 2014). PPAR-γ activation is related to the induction of cell death by apoptosis through the mitochondria. Synthesis of fatty acids of *Novo* is essential for sustaining rapid tumor growth and reprogramming lipid metabolism is a newly recognized hallmark of malignancy (Sugiura, Satoh, & Takasaki, 2021). Mito- SG1, reduced PPAR-γ expression by ~70% in KATO III; in AGS the increase, although not significantly. This reduction may be due to the activity of Mito-SG1 on MAPK and the low response by the cell even though a non-significant increase in AMPK expression is seen. We believe that Mito-SG1 inhibits the synthesis of FA by inhibition of ACC. In the same way, adipose tissue modulates the development and treatment of cancer, affecting the responsiveness to chemotherapy. We found that PPAR-g decreased, reports show that PPAR-g is considered the primary regulator of adipogenesis and, similarly, PPAR-g is downregulated by DXR, reducing glucose absorption and adiponectin concentrations *in vivo*. MAPK signaling pathway is involved in many important cellular processes and is inappropriately activated in many cancers and evidence indicated that ERK inhibitors represent a promising class to target this signaling pathway (Chi et al., 2021). Our results indicate that Mito-SG1 decreased to p-ERK/ERK, indicating that Mito-SG1 could modulate ERK1/2 activity, and consequently, control cell growth, migration, proliferation, differentiation, and apoptosis (Chi et al., 2021). ROS can promote molecular genetic alterations that are necessary for tumor initiation, growth, and progression, as well as the acquisition of resistance to treatment (Lu, Chiang, Tsai, Hsu, & Juan, 2019). Here, we report that Mito-SG1 did not generate significant levels of H_2O_2 in both GC cells, decreased the concentration of the radical $O_2^{\bullet-}$ in AGS cells, and increased SOD levels in KATO III cells. Mito-SG1 reduced ROS levels, probably due to mitochondrial damage, glycolysis, and inhibition of FA synthesis that reduced energy metabolism and led to death in CG cells. Evaluation of synergism showed that the best combination was (Mito-SG1 and 5-FU) which caused a strong synergism effect in AGS and a very strong synergism in KATO III. (Mito-SG1 and DXR) caused an almost additive effect and (Mito-SG1 and Sorafenib) caused a mild synergism effect in AGS and KATO III.

CONCLUSIONS

Mito-SG1 inhibits cell viability, growth, and cell migration in GC. Mito-SG1 induced a dose-dependent decrease in oxygen consumption rate, basal respiration, maximal respiration, respiratory reserve capacity, and ATP production. However, the effects are stronger in AGS than in KATO III. Mito-SG1 strongly affects the ability of AGS to respond to changes in energy demands by targeting mitochondria. Effects were attenuated in KATO III. Mito-SG1 modifies the oxidation rate of the main carbon fuel source to keep the reference OCR by affecting the oxidation rate of glucose and fatty acids in KATO III, but not in AGS, where the rate of glutamine oxidation is affected. Mito-SG1 may be considered an alternative in future studies evaluating the cytotoxic effects of neoplasms to increase treatment selectivity and efficacy. It is also especially important to considerably reduce

the adverse effects associated with these therapies. We propose the evaluation of *in vivo* models with Mito-SG1 and combinations of this drug with 5-FU and Sorafenib. Our results show that Mito-SG1 is a novel alternative for the treatment of CG.

REFERENCES

Batchuluun, B., Pinkosky, S. L., & Steinberg, G. R. (2022). Lipogenesis inhibitors: therapeutic opportunities and challenges. *Nature Reviews Drug Discovery*, *21*(4), 283–305. https://doi.org/10.1038/s41573-021-00367-2

Battogtokh, G., Cho, Y. Y., Lee, J. Y., Lee, H. S., & Kang, H. C. (2018). Mitochondrial-Targeting Anticancer Agent Conjugates and Nanocarrier Systems for Cancer Treatment. *Frontiers in Pharmacology*, *9*. https://doi.org/10.3389/fphar.2018.00922

Boice, A., Bouchier-hayes, L., & Biology, C. (2020). Targeting apoptotic caspases in cancer. *Biochim Biophys Acta*, *6*(1887), 1–39. https://doi.org/10.1016/j.bbamcr.2020.118688.Targeting

Cheng, Y., & Tian, H. (2017). Current Development Status of MEK Inhibitors. *MOLECULES*, *2017*(22). https://doi.org/10.3390/molecules22101551

Cheng, G., Lopez, M., Zielonka, J., Hauser, A. D., Joseph, J., McAllister, D., … Kalyanaraman, B. (2011). Mitochondria-targeted nitroxides exacerbate fluvastatin-mediated cytostatic and cytotoxic effects in breast cancer cells. *Cancer Biology and Therapy*, *12*(8), 707–717. https://doi.org/10.4161/cbt.12.8.16441

Chi, T., Wang, M., Wang, X., Yang, K., Xie, F., & Liao, Z. (2021). PPAR- g Modulators as Current and Potential Cancer Treatments. *Frontiers in Oncology*, *11*(September), 1–17. https://doi.org/10.3389/fonc.2021.737776

Ciccarese, F., Zulato, E., & Indraccolo, S. (2019). LKB1/AMPK Pathway and Drug Response in Cancer: A Therapeutic Perspective. *Oxidative Medicine and Cellular Longevity*, *2019*, 1–16. https://doi.org/10.1155/2019/8730816

Cunniff, B., Benson, K., Stumpff, J., Newick, K., Held, P., Joseph, J., … Heintz, N. H. (2014). *Mitochondrialtargeted nitroxides disrupt mitochondrial architecture and inhibit expression of peroxiredoxin 3 and FOXM1 in malignant mesothelioma cells. 228*(4), 835–845. https://doi.org/10.1002/jcp.24232.Mitochondrial-Targeted

Galluzzi, L., Morselli, E., Kepp, O., Vitale, I., Rigoni, A., Vacchelli, E., … Kroemer, G. (2010).

Mitochondrial gateways to cancer. *Molecular Aspects of Medicine*, *31*(1), 1–20. https://doi.org/10.1016/j.mam.2009.08.002

Gonzalez-Hormazabal, P., Musleh, M., Bustamante, M., Stambuk, J., Pisano, R., Valladares, H., … Berger, Z. (2019). Polymorphisms in RAS/RAF/MEK/ERK pathway are associated with gastric cancer. *Genes*, *10*(1), 1–10. https://doi.org/10.3390/genes10010020

Herzig, S., & Shaw, R. J. (2018). *AMPK: guardian of metabolism and mitochondrial homeostasis.19*(2), 121–135. https://doi.org/10.1038/nrm.2017.95.AMPK

Hung, W Y, Huang, K. H., Wu, C. W., Chi, C. W., Kao, H. L., Li, A. F., … Lee, H. C. (2012). Mitochondrial dysfunction promotes cell migration via reactive oxygen species-enhanced beta5-integrin expression in human gastric cancer SC-M1 cells. *Biochim Biophys Acta*, *1820*(7), 1102–1110. https://doi.org/10.1016/j.bbagen.2012.04.016

Hung, Wen Yi, Huang, K. H., Wu, C. W., Chi, C. W., Kao, H. L., Li, A. F. Y., … Lee, H. C. (2012). Mitochondrial dysfunction promotes cell migration via reactive oxygen species- enhanced β5-integrin expression in human gastric cancer SC-M1 cells. *Biochimica et Biophysica Acta - General Subjects*, *1820*(7), 1102–1110. https://doi.org/10.1016/j.bbagen.2012.04.016

Kalyanaraman, B. (2017). Teaching the basics of cancer metabolism: Developing antitumor strategies by exploiting the differences between normal and cancer cell metabolism. *Redox Biology*, *12*, 833–842. https://doi.org/10.1016/j.redox.2017.04.018

KIM, D. S., MIN, K., & LEE, S. K. (2020). Cell Cycle Dysregulation Is Associated With 5- Fluorouracil Resistance in Gastric Cancer Cells. *Anticancer Research*, *40*(6), 3247–3254. https://doi.org/10.21873/anticanres.14306

Lee, C., Jung, Ã. M., Jung, Ã. I., Heo, J., & Jeong, Ã. Y. H. (2016). *Cumulative Metformin Use and Its Impact on Survival in Gastric Cancer Patients After Gastrectomy*. *263*(1), 96–102. https://doi.org/10.1097/SLA.0000000000001086

Lewandowski, M., & Gwozdzinski, K. (2017). Nitroxides as antioxidants and anticancer drugs. *International Journal of Molecular Sciences*, *18*(11). https://doi.org/10.3390/ijms18112490

Lin, J., He, J., He, X., Wang, L., Xue, M., Zhuo, W., … Chen, S. (2020). HoxC6 Functions as an Oncogene and Isoform HoxC6-2 May Play the Primary Role in Gastric Carcinogenesis. *Digestive Diseases and Sciences*, *65*(10), 2896–2906. https://doi.org/10.1007/s10620-019- 06013-7

Lu, C., Chiang, J., Tsai, F., Hsu, Y., & Juan, Y. (2019). *Metformin triggers the intrinsic apoptotic response in human AGS gastric adenocarcinoma cells by activating AMPK and suppressing mTOR / AKT signaling*. 1271–1281. https://doi.org/10.3892/ijo.2019.4704

Mast, J. M., Hinds, J. W., Tse, D., Axelrod, K., Kuppusamy, M. L., Kmiec, M. M., … Kuppusamy, P. (2020). Selective Induction of Cellular Toxicity and Anti-tumor Efficacy by N-Methylpiperazinyl Diarylidenylpiperidone and its Pro-nitroxide Conjugate through ROS- mediated Mitochondrial Dysfunction and G2/M Cell-cycle Arrest in Human Pancreatic Cancer. *Cell Biochemistry and Biophysics*, *78*(2), 191–202. https://doi.org/10.1007/s12013- 020-00919-0

Matsuoka, T., & Yashiro, M. (2014). The role of PI3K/Akt/mTOR signaling in gastric carcinoma. *Cancers*, Vol. 6, pp. 1441–1463. https://doi.org/10.3390/cancers6031441

Moindjie, H., Rodrigues-Ferreira, S., & Nahmias, C. (2021). Mitochondrial metabolism in carcinogenesis and cancer therapy. *Cancers*, *13*(13). https://doi.org/10.3390/cancers13133311

Neuzil, J., Dong, L., Rohlena, J., Truksa, J., & Ralph, S. J. (n.d.). Mitochondrion Classification of mitocans , anti-cancer drugs acting on mitochondria. *MITOCH*. https://doi.org/10.1016/j.mito.2012.07.112

Paskeh, M. D. A., Saebfar, H., Mahabady, M. K., Orouei, S., Hushmandi, K., Entezari, M., … Samarghandian, S. (2022). Overcoming doxorubicin resistance in cancer: siRNA-loaded nanoarchitectures for cancer gene therapy. *Life Sciences*, *298*(March), 120463. https://doi.org/10.1016/j.lfs.2022.120463

Pauligk, C., Homann, N., Kopp, H., Haag, G. M., Folprecht, G., Probst, S., … Essen, H. (2017). Docetaxel, oxaliplatin, and fluorouracil/leucovorin (FLOT) for resectable esophagogastric cancer: Updated results from multicenter, randomized phase 3 FLOT4-AIO trial (German Gastric Group at AIO). *Annals of Oncology*, *28*(v616). https://doi.org/https://doi.org/10.1093/annonc/mdx440.019

Refolo, M. G., Lotesoriere, C., Lolli, I. R., Messa, C., & D'Alessandro, R. (2020). Molecular mechanisms of synergistic action of Ramucirumab and Paclitaxel in Gastric Cancers cell lines. *Scientific Reports*, *10*(1), 1–13. https://doi.org/10.1038/s41598-020-64195-x

Riquelme, I., Tapia, O., Espinoza, J. A., Leal, P., Buchegger, K., Sandoval, A., … Roa, J. C. (2018). The Gene Expression Status of the PI3K/AKT/mTOR Pathway in Gastric Cancer Tissues and Cell Lines. *Pathology and Oncology Research*, *22*(4), 797–805. https://doi.org/10.1007/s12253-016-0066-5.The

Salaroglio, I. C., Mungo, E., Gazzano, E., Kopecka, J., & Riganti, C. (2019). ERK is a Pivotal Player of Chemo-Immune-Resistance in Cancer. *International Journal of Molecular Sciences*, *20*(10), 1–31.

Shen, Y., Yang, J., Li, J., Shi, X., Ouyang, L., Tian, Y., & Lu, J. (2014). Carnosine inhibits the proliferation of human gastric cancer SGC-7901 cells through both of the mitochondrial respiration and glycolysis pathways. *PLoS One*, *9*(8), e104632. https://doi.org/10.1371/journal.pone.0104632

Snezhkina, A. V, Kudryavtseva, A. V, Kardymon, O. L., Savvateeva, M. V, Melnikova, N. V, Krasnov, G. S., & Dmitriev, A. A. (2019). Review Article ROS Generation and Antioxidant Defense Systems in Normal and Malignant Cells. *Oxidative Medicine and Cellular Longevity*, *2019*.

Sugiura, R., Satoh, R., & Takasaki, T. (2021). ERK: A Double-Edged Sword in Cancer. ERK- Dependent Apoptosis as a Potential Therapeutic Strategy for Cancer. *Cells*, *2021*(10).

Sung, H., Ferlay, J., Siegel, R. L., Laversanne, M., Soerjomataram, I., Jemal, A., & Bray, F. (2021). Global Cancer Statistics 2020: GLOBOCAN Estimates of Incidence and Mortality Worldwide for 36 Cancers in 185 Countries. *CA: A Cancer Journal for Clinicians*, *71*(3), 209–249. https://doi.org/10.3322/caac.21660

Tan, Y. en, Wang, P. liang, Yin, S. cheng, Zhang, C., Hou, W. bin, & Xu, H. mian. (2020). Thirty- year trends in clinicopathologic characteristics and prognosis after gastrectomy for gastric cancer: A single institution in Northern China. *Journal of Cancer*, *11*(5), 1056–1062. https://doi.org/10.7150/jca.36927

Tarasiuk, O., Miceli, M., & Domizio, A. Di. (2022). AMPK and Diseases : State of the Art Regulation by. *Biology*, *11*(1041).

Vlq, K. U., Ri, P., Lgdwlyh, S., Ri, Q., & Santos, J. (2012). Cytotoxic Effects of Mitochondria- Targeted Nitroxide Mito-SG1 on Hepatic Cancer Cells. *Free Radical Biology and Medicine*, *53*, S50. https://doi.org/10.1016/j.freeradbiomed.2012.10.134

Wang, H., Wang, A., Wang, X., Zeng, X., & Xing, H. (2022). AMPK/PPAR-γ/NF-κB axis participates in ROS-mediated apoptosis and autophagy caused by cadmium in pig liver. *Environmental Pollution*, *294*(September 2021), 118659. https://doi.org/10.1016/j.envpol.2021.118659

Wang, W., Chen, S., Huang, H., & Juan, H. (2021). Proteomic Analysis Reveals That Metformin Suppresses PSMD2, STIP1, and CAP1 for Preventing Gastric Cancer AGS Cell Proliferation and Migration. *ACS Omega*, *6*(22), 14208–14219. https://doi.org/10.1021/acsomega.1c00894

Yu, C., Wu, X., Yao, B., & Tao, H. (2019). Silencing of acetyl-CoA carboxylase-α gene in human gastric cancer cells inhibits proliferation via induction of apoptosis, autophagy and suppression of cell invasion. *Tropical Journal of Pharmaceutical Research*, *18*(10), 2025– 2030. https://doi.org/10.4314/tjpr.v18i10.4

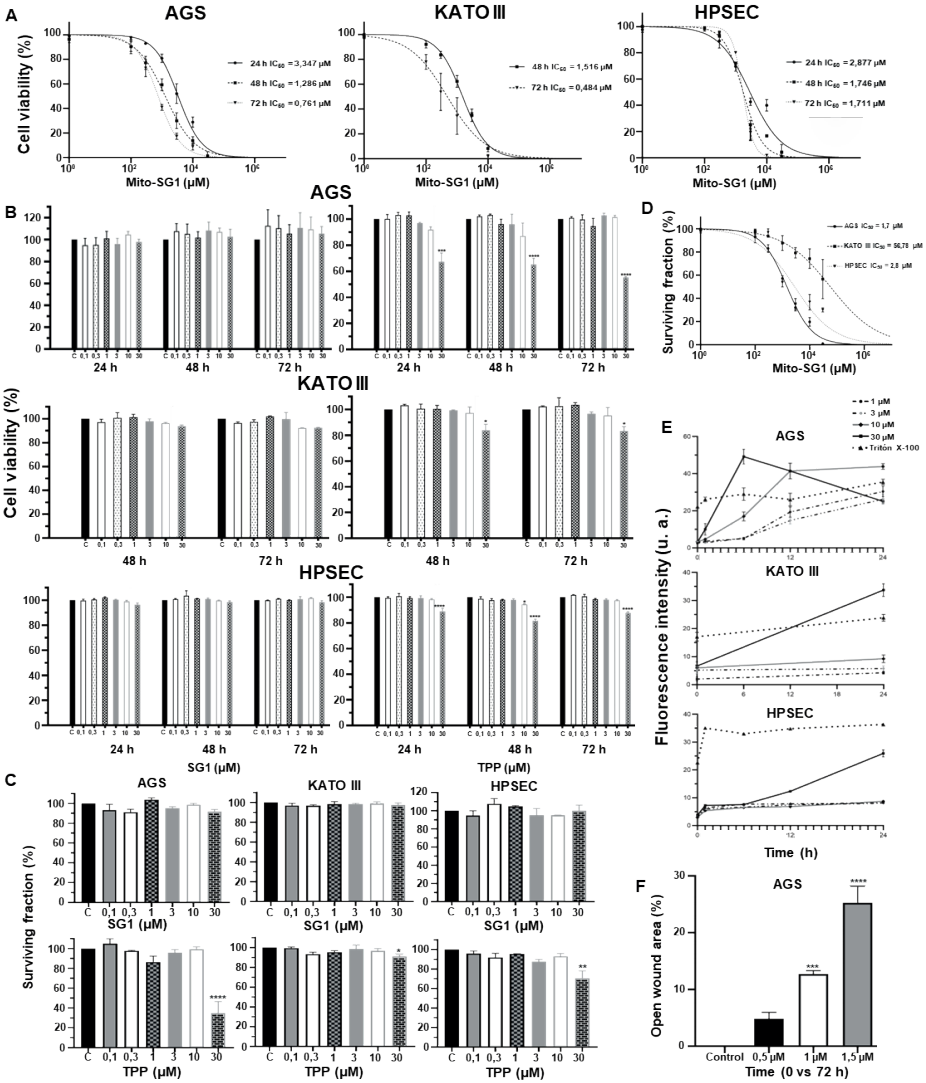

Figure 1. The cytotoxicity of Mito-SG1 significantly affected CG cell lines. A. Evaluation of cell viability in cell lines that were treated with Mito-SG1 during 24, 48 and 72 by means of the MTT assay. B. Evaluation of cell viability in cell lines that were treated with TPP and SG1 during 24, 48 and 72 by means of the MTT assay. C. Determination of the survival fraction of cell lines pretreated for 24 h with TPP and SG1. D. Determination of the survival fraction of cell lines pretreated for 24 h with Mito-SG1. E. Real-time detection of cell death in cell lines pretreated with Mito-SG1 for 24 h. F. Evaluation of cell migration in AGS pretreated for 24 hours with Mito-SG1. Data are presented as % of control +/- ESM. *p < 0.05; **p < 0.01; p<0.001; p<0.0001. n=3, representative data from three independent experiments.

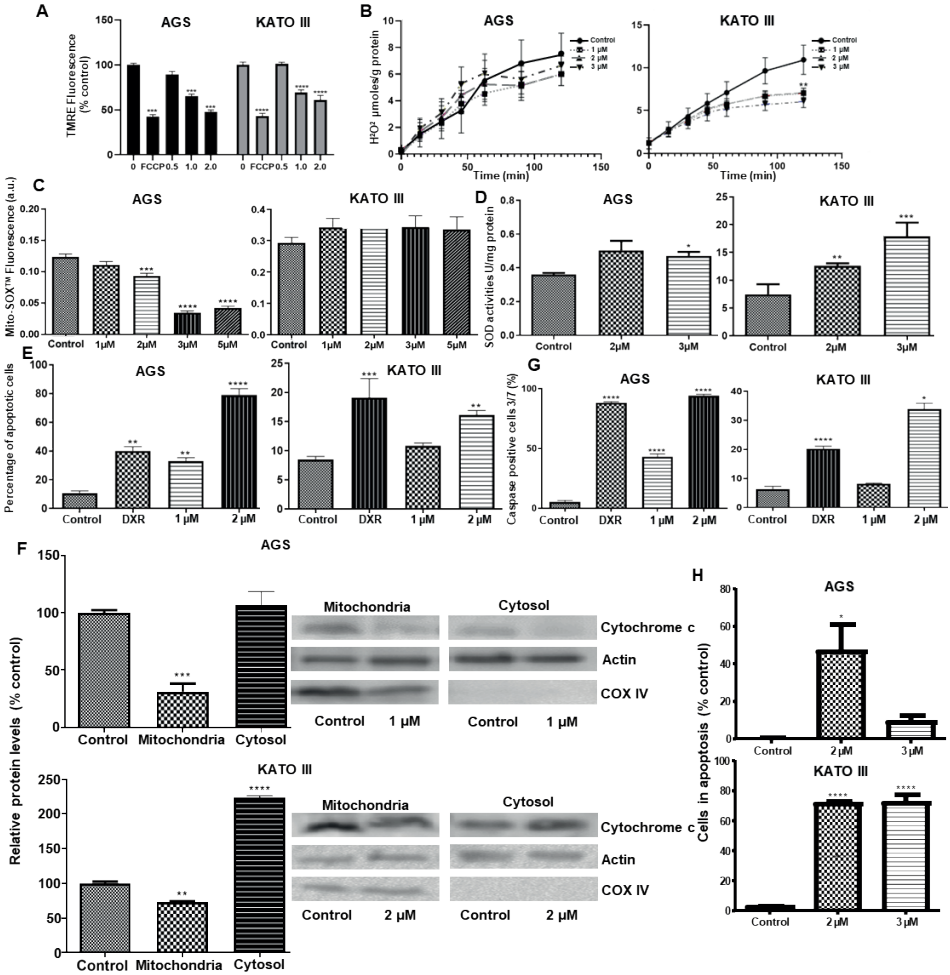

Figure 2. Mito-SG1 leads the loss of mitochondrial structural integrity inducing cell death by apoptosis in AGS and KATO III. A. Mitochondrial membrane potential was measured with TMRE by spectroscopy. B. H2O2 levels were determined with Amplex Red by spectroscopy. C. Mitochondrial ROS were determined with Mito-SOX™ Red by fluorescence microscopy. D. SOD activity was measured using a Trevigen superoxide dismutase kit. And. Apoptotic cells were detected by the Apopxin assay with the apoptosis/necrosis kit (abcam). F. Cytochrome c release was detected by Western blot transfer. G. Caspase-3/7 was analyzed by flow cytometry. H. DNA integrity was assessed using the TUNEL assay. Data are presented as % of control +/- ESM. *p < 0.05; **p < 0.01; p<0.001; p<0.0001. n=3, representative data from three independent experiments.

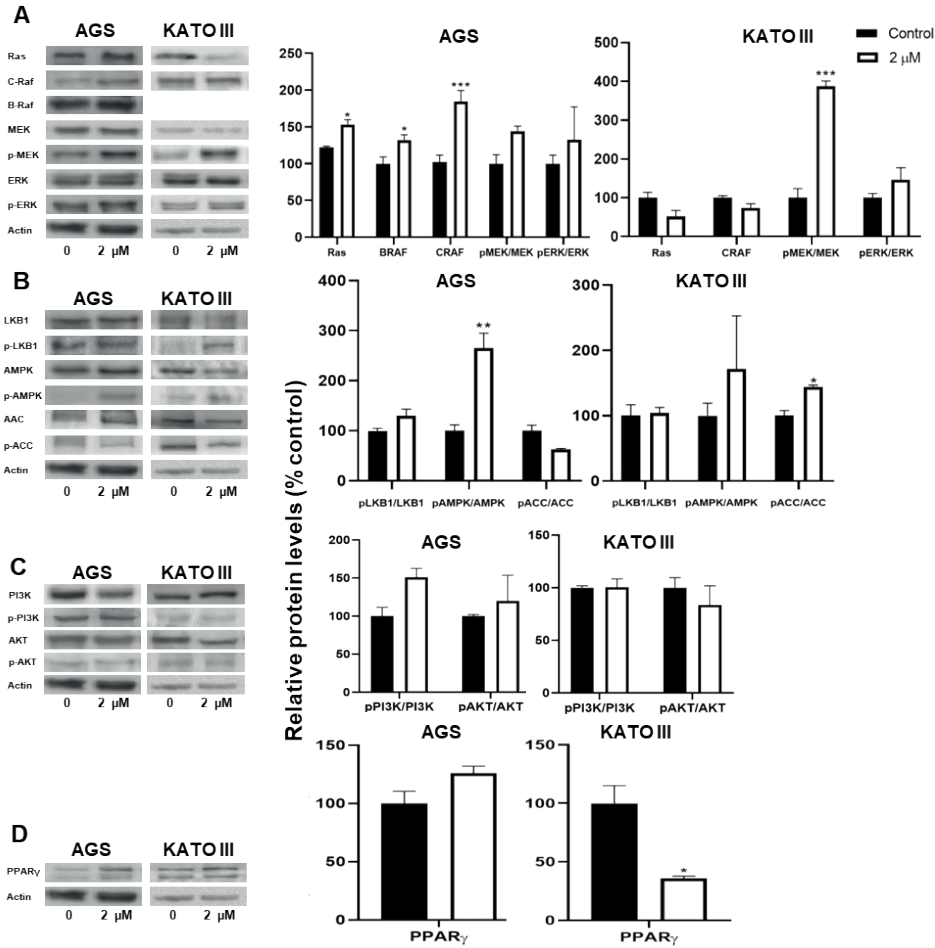

Figure 3. Mito-SG1 affects the expression of signaling pathways in AGS and KATO. A. The effect of Mito-SG1 on the RAS/RAF/MEK/ERK pathway by Western Blot transfer was analyzed. B. The effect of Mito-SG1 on the LKB1/AMPK/ACC pathway by Western Blot transfer was analyzed. C. The effect produced by Mito-SG1 on the PI3K/AKT pathway by Western Blot transfer was analyzed. D. The effect produced by Mito-SG1 on the PPARγ pathway by Western Blot transfer was analyzed. Data are presented as % of control +/- ESM. *p < 0.05; **p < 0.01; p<0.001; p<0.0001. n=3, representative data from three independent experiments.

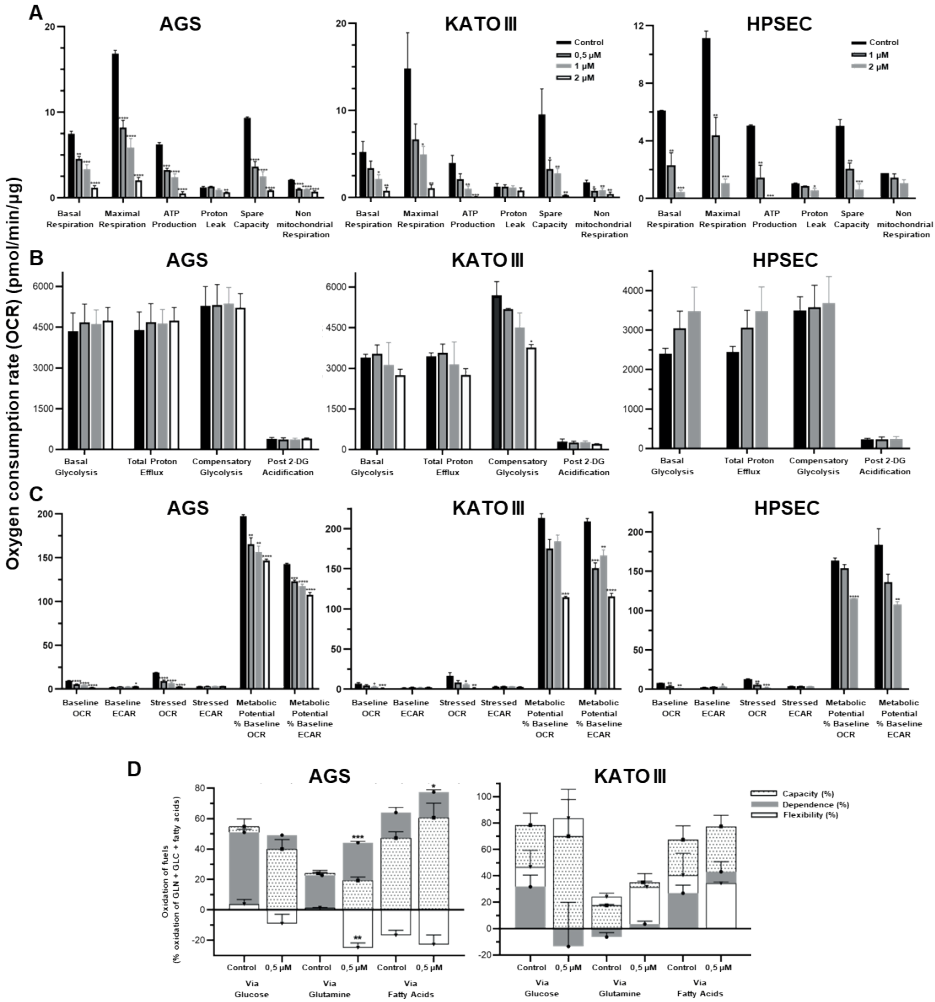

Figure 4. Mito-SG1 affects mitochondrial bioenergetics in AGS and KATO III cells. The effects produced by Mito-SG1 on cell lines were evaluated in real time by means of the extracellular flow analyzer XFe24 (Seahorse Bioscience, Billerica, MA). A. The effects produced on the rate of oxygen consumption in cells that were previously stressed for 24 h with different concentrations of Mito-SG1 were analyzed. B. The effects produced on the glycolytic rate in cells that were previously treated for 24 h with different concentrations of Mito-SG1 were analyzed. C. The effects on metabolic potential were evaluated after 24 h of treatment with different concentrations of Mito-SG1 in all cell lines. D. The parameters (capacity, dependence and flexibility) in the cells that were treated for 24 h with different concentrations of Mito-SG1 were evaluated to know the response of the cells to the inhibition of carbon sources used by mitochondria in their energy functions. Data are presented as mean +/- ESM, n≥3, *p < 0.05; **p < 0.01; p<0.001; p<0.0001.)

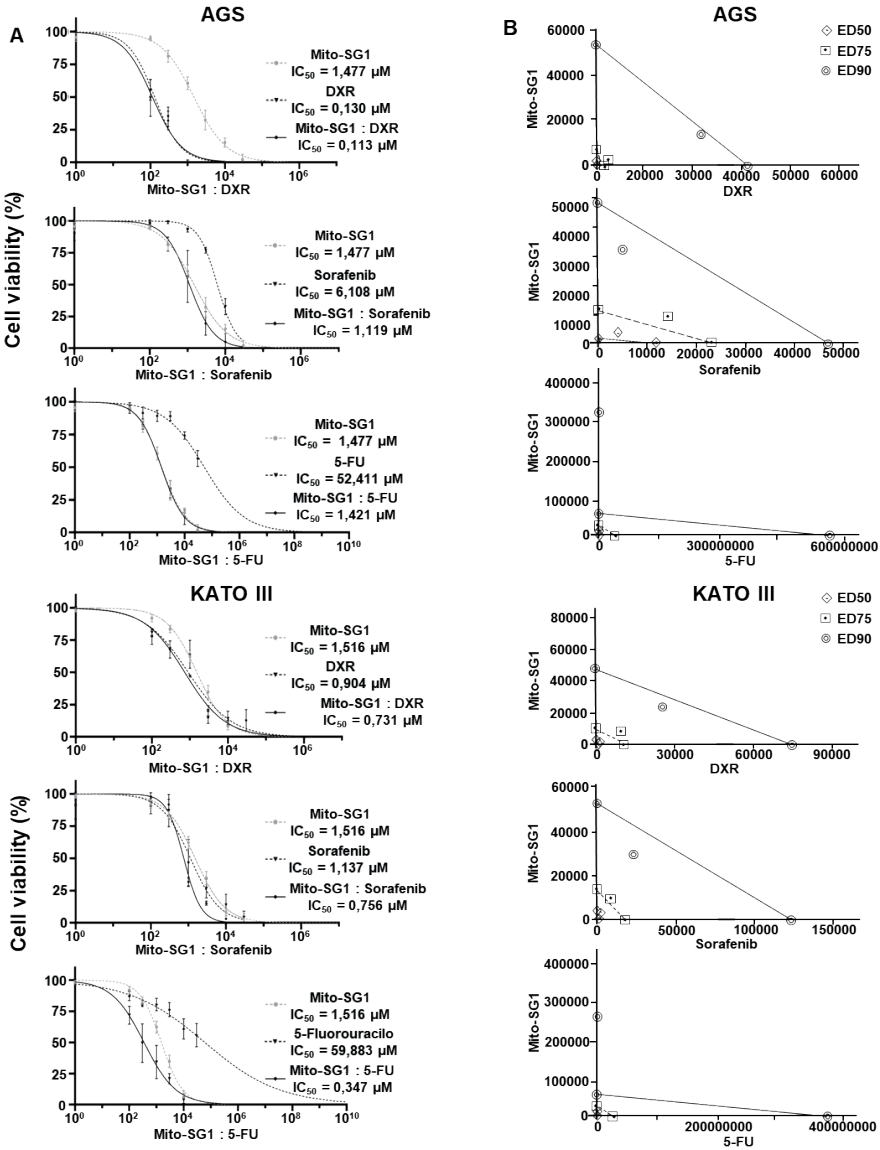

Figure 5. Mito-SG1 strongly potentiates the antineoplastic effect of 5-Fluorouracil in KATO III and produces an almost additive effect with sorafenib in AGS and KATO III. A. Evaluation of the cytotoxicity of the pharmaceutical combinations, Mito-SG1 and Doxorubicin, Mito-SG1 and Sorafenib, Mito-SG1 and 5-Fluorouracil, used for the treatment of CG AGS and KATO III cell lines for 48 h. B. The isobolograms of each of the pharmaceutical combinations are presented according to their IC50, IC75 and IC90 values. of Data are presented as mean +/- ESM, n≥3, *p < 0.05; **p < 0.01; p<0.001; p<0.0001.)